axial symmetry. It is feasible that trial solutions of this problem could consist of the sum of axisymmetric solutions and solutions that are periodic in the azimuthal angle; biharmonic functions with these properties are well known.

A formulation that utilizes as many standard solutions as possible is essential to advanced applications of techniques that rely on closed-form solutions. The Galerkin stress functions probably admit more standard solutions than any other formulation, but the literature apparently lacks a simple direct derivation of these functions under conditions that are just sufficiently general to cover engineering applications. Ordinarily, stress functions are obtained inversely, but recently De La Penha and Childs[2] derived the axisymmetric Love stress function directly from the equations of equilibrium. In this Note the Galerkin stress functions will be derived directly from Navier's equations for the fully three-dimensional case, assuming a finite body. The Love stress function emerges as a special case for axial symmetry in cylindrical coordinates.

Let the body occupy a finite region, R, bounded by an outer closed surface which may contain inner closed surfaces. Let the displacement vector, $\mathbf{u}$, be a point function that, along with its derivatives, is single valued, finite and continuous in R and vanishes outside R. With $\alpha = 2(1 - \nu)/(1 - 2\nu)$ (ν = Poisson's ratio), the homogeneous parts of Navier's equations[3] may be written

$$\nabla^2\mathbf{u} + (\alpha - 1)\,\text{grad div}\mathbf{u} = \mathbf{0} \tag{1}$$

By Helmholtz's theorem[4] there exist ϕ and $\mathbf{V}$ such that

$$\mathbf{u} = A(\text{grad}\phi - \alpha\,\text{curl}\mathbf{V}) \tag{2}$$

where A ($\neq 0$) is an arbitrary constant. The representation Eq. (2) is not unique, because ϕ is defined only up to a constant and $\mathbf{V}$ is defined only up to a gradient vector. So without loss of generality, put

$$\mathbf{V} = \text{curl}\mathbf{U} \tag{3}$$

It is required to express ϕ generally in terms of $\mathbf{u}$. Evidently $\mathbf{u}$ is unaffected by the addition of an arbitrary gradient vector to $\mathbf{U}$. This gradient vector can be chosen so that

$$\phi = \text{div}\mathbf{U} \tag{4}$$

for if $\mathbf{U} = \mathbf{U}' + \text{grad}W$, then $\phi = \text{div}\mathbf{U}' + \nabla^2 W$ and the validity of Eq. (4) rests on the solution of Poisson's equation. From the conditions imposed on $\mathbf{u}$ and the relationships of ϕ and $\mathbf{U}$ to $\mathbf{u}$, ϕ and div$\mathbf{U}'$ must be finite and continuous in R and may be set equal to zero outside R, hence the standard solution,

$$W = (4\pi)^{-1} \iiint_R r^{-1}(\text{div}\mathbf{U}' - \phi)dV$$

is valid. Equations (2–4) give

$$\mathbf{u} = A(\text{grad div}\mathbf{U} - \alpha\,\text{curl curl}\mathbf{U})$$

hence

$$\mathbf{u} = A[\nabla^2\mathbf{U} - (\alpha - 1)\,\text{curl curl}\mathbf{U}] \tag{5}$$

On substituting $\mathbf{u}$ from Eq. (5), Eq. (1) reduces to $A\,\alpha\,\nabla^4\mathbf{U} = \mathbf{0}$. The case $\nu = \frac{1}{2}$ may be included by choosing $A = 2\nu - 1$, so for $\nu \neq 1$

$$\nabla^4\mathbf{U} = \mathbf{0} \tag{6}$$

and Eq. (5) becomes

$$\mathbf{u} = \text{grad div}\mathbf{U} - 2(1 - \nu)\nabla^2\mathbf{U} \tag{7}$$

Equation (7) [subject to Eq. (6)] is the Galerkin solution. In Cartesian coordinates the components of Eq. (6) are the biharmonic Galerkin stress functions. In cylindrical coordinates, r, θ, z with unit vectors $\mathbf{a}$, $\mathbf{b}$, $\mathbf{c}$, respectively, let $\mathbf{U} = U_1\mathbf{a} + U_2\mathbf{b} + U_3\mathbf{c}$. Then

$$\text{div}\mathbf{U} = \partial U_1/\partial r + U_1/r + r^{-1}\partial U_2/\partial\theta + \partial U_3/\partial z$$

and

$$\nabla^2\mathbf{U} = \{\nabla^2 U_1 - U_1/r^2 - 2r^{-2}\partial U_2/\partial\theta\}\mathbf{a} + \{2r^{-2}\partial U_1/\partial\theta + \nabla^2 U_2 - U_2/r^2\}\mathbf{b} + \nabla^2 U_3\mathbf{c}$$

So if $U_1 = U_2 = \partial U_3/\partial\theta = 0$, the solution reduces to the axisymmetric solution with U_3 as the Love stress function.

The conditions imposed on R and $\mathbf{u}$ are not the most general for which the Galerkin solution is valid, but the preceding direct derivation applies to most situations of practical interest. The transformation[3] of the Galerkin solution to the Neuber–Papkovich solution is insufficient to establish generality, because the expression

$$\mathbf{u} = \text{grad div}\mathbf{U} - (1 - 2\nu)\,\text{grad}F - 2(1 - \nu)\nabla^2\mathbf{U}$$

also satisfies Eq. (1) provided that $\nabla^2(\nabla^2\mathbf{U} + \text{grad}F) = \mathbf{0}$, and similarly may be transformed to the Neuber–Papkovich solution. It is not obvious that F is disposable. For $\nu = \frac{1}{2}$, $\mathbf{u}$ does not contain F, but div$\mathbf{u} = (2\nu - 1)\nabla^2(\text{div}\mathbf{U} + F)$, and the limit as $\nu \to \frac{1}{2}$ of div$\mathbf{u}/(1 - 2\nu)$ occurs in the linear expressions for the direct stresses.

References

[1] Wallis, F. R., "Stress Analysis of Solid-Propellant Rocket Charges by Point Matching," *Journal of Spacecraft and Rockets*, Vol. 6, No. 9, Sept.. 1969, pp. 1082–1084.

[2] De La Penha, G. and Childs, B., "A Note on Love's Stress Function," *AIAA Journal*, Vol. 7, No. 3, March 1969, pp. 540.

[3] Sokolnikoff, I. S., *Mathematical Theory of Elasticity*, 2nd ed., McGraw-Hill, New York, 1956, pp. 73 and 334.

[4] Weatherburn, C. E., *Advanced Vector Analysis*, G. Bell and Sons, London, 1954, pp. 44.

One-Dimensional Theory of Monopropellant Rocket Combustion

V. K. Jain* and N. Ramani†

Indian Institute of Science, Bangalore, India

Nomenclature

A = $\dot{m}''_f rc/k \ln(1 + B)$
B = transfer number, $c(T_b - T_s)/Q$
a,b = coefficients in ξ^* expression, Eq. (11)
c = constant pressure heat capacity
D = diameter of the droplet
G = mass flow rate at injection per unit duct area
k = thermal conductivity of the gas
$\dot{m}''_f$ = mass flow rate per unit area in a plane laminar flame
$\dot{m}''_s$ = mass flow rate per unit area at the droplet surface
Pr = Prandtl number
P = exponent in ξ^* expression, Eq. (11)
Q = latent heat of vaporization of the propellant
Re_0 = Reynolds number, $2Gr_0/\mu$
r = droplet radius
T_b = adiabatic burnt temperature
T_s = droplet surface temperature
t = time
u,v = gas velocity and droplet velocity, respectively
W = $\rho u/G$
x = axial distance
ζ = r/r_0
μ = viscosity of the gas

Received December 10, 1969. The authors thank H. S. Mukunda for discussions and the authorities of TIFR, Bombay, for the CDC-3600 Computer facility provided.

* Associate Professor, Department of Aeronautical Engineering.

† Senior Research Assistant, Department of Aeronautical Engineering.

$\xi = k \ln(1 + B)\rho x/r_0^2 c\rho_l G$; $\xi^{*\prime} = 2\rho x^*/(\mathrm{Pr})\rho_l$
ρ, ρ_l = densities of gas and liquid, respectively
$\chi = \rho v/G$

Subscript

o = state at injector plane

Superscript

* = condition when the droplets disappear

Introduction

ALTHOUGH combustion in a bipropellant rocket motor is rather well understood (see, e.g., Refs. 1–4), similar progress in the case of monopropellant rocket motors seems lacking, perhaps due to the involved burning rate dependence on the droplet radius. In this Note we consider the problem of monopropellant rocket combustion under some idealized conditions. Using the burning rate expression given by the "thin-flame" model of Spalding and Jain,[5] the governing equation is obtained for the decrease of the droplet radius r. Considering the process of droplet drag and the conservation of mass, governing equations for droplet velocity v and gas velocity u are written. The equations are cast in dimensionless form and integrated numerically to obtain the variations of u, v, and r along the combustion chamber length under various initial conditions and chamber pressures. The length of the combustion chamber required for the droplets to disappear completely is obtained for the case of hydrazine droplets. Based on the numerical results obtained, an expression for the combustion chamber length is suggested as a function of the parameters involved, namely, injection velocity, initial droplet size, transfer number, and Reynolds number. This simple expression agrees with the numerical results to an accuracy of about 7% in the practical range of parameters.

Formulation

We consider an idealized rocket motor wherein droplets of uniform size are injected with a uniform velocity v_0. As they move through the chamber, they decrease in diameter as a result of combustion, and, therefore, the gas mass flow rate increases from zero at the injector plane to a maximum at the plane where the droplets finally disappear. The droplets are initially slowed down by friction with the gas, and as u begins to exceed v as a result of droplet vaporization and combustion, the droplets are accelerated once again. Finally, as the droplets disappear, $v \to u$.

It is assumed that the process is steady, adiabatic and one-dimensional. The state of the gas is taken to be that of combustion products of monopropellant in equilibrium, and turbulent mixing in the longitudinal direction and the kinetic energy of motion are neglected. Under these conditions the governing equations take the following form.

The decrease of the droplet radius is given by[5]:

$$v(dr/dx) = -(k/c\rho_l) \ln(1 + B)(\alpha/r)\varphi \tag{1}$$

$$\alpha \equiv [2 + A + (A^2 + 4A)^{1/2}]/2 \tag{2}$$

$$\varphi \equiv [1 + 0.276(\rho|u - v|D/\mu)^{1/2}\mathrm{Pr}^{1/3}] \tag{3}$$

where φ is to account for the forced convection.[6]

The change of droplet velocity is governed by[4]:

$$v(dv/dx) = (9/2)(\mu/r^2)(u - v)\Phi\varphi \tag{4}$$

where the factor, $\Phi \equiv (\dot{m}''_s rc/k)/(e^{\dot{m}''_s rc/k} - 1)$, is to correct for the reduction in drag due to outward mass transfer.[2]

The mass conservation equation can be written as

$$\rho u = G(1 - r^3/r_0^3) \tag{5}$$

Introducing the following dimensionless transformations: $\zeta = r/r_0$, $\chi = \rho v/G$, $\xi = (k/r_0^2 c\rho_l G)\rho x \ln(1 + B)$, $W = \rho u/G = 1 - \zeta^3$, and $Re_0 = 2Gr_0/\mu$, the governing equations

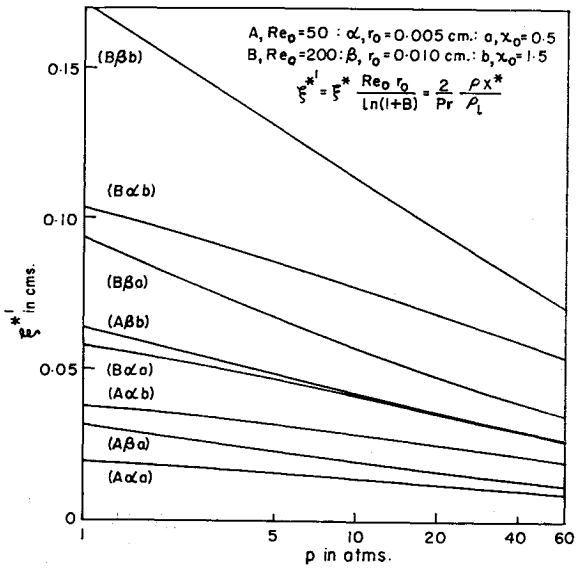

Fig. 1 The variation of ξ with p.

are rewritten for the purpose of numerical integration as

$$(d\zeta^2/d\xi) = -(2\alpha/\chi)[1 + 0.245(Re_0|W - \chi|\zeta)^{1/2}] \tag{6}$$

$$\frac{d\zeta^2\chi}{d\xi} = \chi\frac{d\zeta^2}{d\xi} + 3.15(W - \chi)[1 + 0.245 \times (Re_0|W - \chi|\zeta)^{1/2}][\alpha/\{(1 + B)^\alpha - 1\}\chi] \tag{7}$$

where Pr = 0.7 has been used which is true for most gases, and

$$A = A_0\zeta \tag{8}$$

The initial conditions are

$$\xi = 0: \zeta^2 = 1, \zeta^2\chi = \chi_0 \tag{9}$$

For a given propellant and chamber pressure we obtain B and A/r from Ref. 5, and the choice of the initial droplet size r_0 specifies A_0. Fixing the values of injection velocity χ_0 and Reynolds number Re_0 determines the initial condition and the parameters involved in the problem. The variations of droplet radius, droplet velocity and gas velocity are obtained along the combustion chamber length by numerically integrating the differential Eqs. (6) and (7) with the initial conditions Eq. (9) and using Eq. (8). ξ^*, the value of ξ where $\zeta = 0$, is also obtained; it is the dimensionless combustion chamber length.

Results and Discussion

Figure 1 presents $\xi^{*\prime}$ for hydrazine for $\chi_0 = 0.5$ and 1.5, $Re_0 = 50$ and 200, $r_0 = 0.005$ and 0.01 cm, and $1 \leq p \leq 60$ atm. Here $\xi^{*\prime}$ is a modified combustion chamber length,

$$\xi^{*\prime} = 2\rho x^*/\mathrm{Pr}\rho_l = \xi^* Re_0 r_0/\ln(1 + B) \tag{10}$$

From Fig. 1, it is seen that as pressure increases, $\xi^{*\prime}$ decreases, and hence more so the combustion chamber length decreases. Furthermore, this effect of pressure seems to be larger for larger values of each of the parameters χ_0, r_0, and Re_0.

The plot of ξ^* vs A_0 (not shown here), A_0 being varied by varying p, was found to be insensitive to r_0 variations, the other parameters having specified values. This leads to the conclusion that the ξ^* vs A_0 relationship is almost unaffected by p and r_0 variations; however, both ξ^* and A_0 depend on p and r_0. In other words, other parameters being fixed, A_0 specifies ξ^*, no matter what combination of p and r_0 gives this A_0.

A systematic and detailed study of the dependence of ξ^* on the parameters in the case of hydrazine led to the following

correlation:

$$\xi^* = (a\chi_0 + b)(1 + 0.245Re_0^{1/2})^P \quad (11)$$

where

$$a = 0.504(2.0 + A_0)^{0.440}$$
$$b = 0.177(1.5 + A_0)^{0.107}$$

and

$$P = 1.29 - 0.815/\chi_0 \quad \chi_0 \geq 1$$
$$= 0.462 + 0.013/\chi_0 \quad \chi_0 \leq 1$$

This relationship for ξ^* agrees with the numerical results obtained within 7%.

References

[1] Priem, R. J., "Propellant Vaporization as a Criterion for Rocket Engine Design; Calculations Using Various Log-Probability Distributions of Heptane Drops," TN 4098, 1957, NACA.

[2] Spalding, D. B., "Combustion in Liquid-Fuel Rocket Motors," *The Aeronautical Quarterly*, Vol. X, 1959, pp. 1–27.

[3] Lambris, S., Comb, L. P., and Levine, R. S., "Stable Combustion Process in Liquid Propellant Rocket Engines," *Fifth AGARD Combustion and Propulsion Colloquium*, Braunschweig, 1962, pp. 569–636.

[4] Williams, F. A., "Progress in Spray-Combustion Analysis," *Eighth International Symposium on Combustion*, Williams and Wilkins, Baltimore, 1962, pp. 50–69.

[5] Spalding, D. B. and Jain, V. K., "Theory of the Burning of Monopropellant Droplets," ARC 20, 176-CF 441-R 436, 1958, Aeronautical Research Council.

[6] Frössling, N., *Beiträge zur Geophysik*, Vol. 52, 1938, p. 170.

Thermal Mission Analysis for the Lunar Module

GUNTER W. GEORGI*

Grumman Aerospace Corporation, Bethpage, N.Y.

THERMAL mission analysis for the Apollo Lunar Module (LM) uses the Grumman Thermal Analyzer (GTA), a Fortran program for the IBM 360/75. This program operates on basic LM ascent-stage and descent-stage thermal networks, which have ~700 and 400 lumped-mass nodes, respectively; most of these nodes are conductively and radiatively coupled with several other nodes. A mission consists of numerous timeline events, among which the thermal events (window shade deployments, hatch openings, rocket engine firings, electronic equipment actuations, etc.) are called parameter changes, since they are accomplished by defining new values for some of the basic parameters: conductors, radiators, and heat sources. In general, a thermal network is defined at the time of a parameter change, and the GTA calculates the transient thermal response until the next parameter change.

For a typical Apollo mission, ~5000 data cards for these parameter changes are used for the LM ascent stage. Since one mispunched or misplaced card can invalidate a computer run, thermal mission analysis is confronted with a serious data handling problem. One approach to reduce the amount of data to manageable levels was to reduce the size of the thermal networks.[1] These simplified networks were found to be useful tools for rapid parametric design analyses. Both simplified and basic networks have been verified by full-scale thermal vacuum testing (for earth orbital and lunar landing missions) as well as by previous Apollo flights. For manned missions, however, the analyses are performed with the basic thermal networks, since a much greater level of detail is required. Thus, it became necessary to take another approach —namely to automate and link the generation, manipulation, and interpretation of data. This approach is the one described in this Note.

Received January 12, 1970.

* Thermodynamics Engineer. Member AIAA.

Thermal Mission Analysis

Thermal mission analysis is accomplished in three steps: 1) the generation of detailed mission timeline data by T-CUP (Timeline and Consumable Usage Program),[2] 2) scanning this data for thermal significance by TSP (Timeline Scanning Program), and 3) the determination of thermal mission constraints by the GTA.

The T-CUP details every planned functional change with respect to time for the anticipated mission. Thus, timeline data concerning astronaut activity schedules, consumable budgets and other mission related data are available (nearly in real time) to prepare and modify the various LM mission timelines (both nominal and contingency) and to determine the usage of expendables. To establish total electrical power consumption, T-CUP generates the usage mode of every equipment on the LM. This detailed mode history of 125 pieces of equipment as well as relevant astronaut/spacecraft activity and consumables are recorded on an output tape (Thermdmp).

The TSP searches the T-CUP output tape for thermal events such as rocket engine firing duration, cabin pressurization, fan operation, glycol coolant loop operation, and equipment on-off switching related to heat dissipations in order to determine times for parameter changes for the GTA program. With these times established, the TSP time-averages the equipment heat loads for the duration of the parameters and transmits this information as well as other thermal data (i.e., rocket engine firing, etc.) to the GTA by means of a compatible output tape. Some equipments have as many as 8 modes of operation and a particular mode may yield heat inputs to as many as 13 network nodes. Also, a particular network node may receive heat input from several different equipments. For a typical mission, over 3000 data cards were required previously to represent all equipment heat input changes. The TSP yields even more detailed information on its Thermdmp output tape (totally eliminating keypunch and card handling errors) as well as defining function control variables (described below) for other thermally significant events.

Thermal mission constraints can be found from the output of the GTA. The thermal data of the TSP output tape together with the basic network representation and typically 30 cards (primarily launch conditions, thermal blanket insulation effectiveness, and spacecraft orientation with respect to the sun-earth-moon at various mission times) serve as input to the GTA. The printed output of lumped-mass-node temperature histories and vehicle heat fluxes, as well as CRT data display curves, can be used to determine if thermal specification limits have been exceeded.

To improve the data handling capability of the GTA, it was recognized that a complex thermal network in principle is identical to a simple analytical model that is suitable for hand calculations. However, with the more complex model it is usually necessary to do many operations for which one suffices in the simple model. Since many thermal events require fixed blocks of data (i.e., combinations of temperatures, masses, conductors, radiators, and heat sources) they can be handled with subroutines triggered by only one variable. With the addition of data handling subroutines to the GTA, it is now possible to control about 25 thermal events for the ascent stage network and 20 events for the descent stage network through single function control variables. (For an ascent stage rocket engine control variable specified as "327," the GTA subroutines will consider this to be a 327-sec engine